Iron(III) Complexation by New Aminocarboxylate Chelators – Thermodynamic and Kinetic Studies

Guy Serratrice,*[a] Jean-Baptiste Galey,[c] Eric Saint Aman,[b] and Jacqueline Dumats[c]

Keywords: Iron / Chelates / Thermodynamics / Kinetics / N ligands

The complexation of Fe^{III} by new tetradentate and pentadentate aminocarboxylate chelators, designed to protect cells against iron-catalysed oxidative damage, was investigated. Ferric iron complexes of *N*,*N*′-bis(3,4,5-trimethoxybenzyl)-ethylenediamine-*N*,*N*′-diacetic acid (**L1**), *N*,*N*′-dibenzylethylenediamine-*N*,*N*′-diacetic acid (**L2**) and [*N*-(2-hydroxybenzyl)-*N*′-benzylethylenediamine-*N*,*N*′-diacetic acid] (**L3**) have been characterized in aqueous solution by potentiometric, UV/Vis spectrophotometric and cyclic voltammetric measurements. The parent ligand, ethylenediamine-*N*,*N*′-diacetic acid (**L4**), has also been studied. As expected, the presence of a hard phenolate donor group in **L3** significantly enhances the affinity for iron while decreasing the potential of the Fe^{III}/Fe^{II} redox couple compared to **L1** or **L2**. Kinetics studies have provided the kinetic rate constants related to the formation and the dissociation of the ferric complex with **L3**. The results reveal a fast Fe^{III} uptake, which is a favorable feature for a biological use of this type of ligand. Overall, these results demonstrate the pertinence of the use of such ligands to protect biological tissues against oxidative stress.

Introduction

In recent years there has been an intensive search for new iron ligands with medicinal applications. Several diseases are indeed associated with disturbance of iron homeostasis.[1] One major issue is the treatment of iron-overload-associated situations for people suffering from haematological defects such as β-thalassemia major. Indeed, because man is unable to actively excrete iron, systemic iron overload occurs rapidly when frequent blood transfusions are given.[2] In such situations, treatment with powerful iron chelators is the only effective way to remove excess iron. Currently, the hexadentate siderophore desferrioxamine (DFO) is by far the clinically most used iron chelator. However, DFO lacks oral activity and has a very short biological half life, which results in poor patient compliance.[3] Therefore, considerable effort has been focused on discovering new therapeutically useful iron chelators.

On the other hand, there are also other areas in which iron chelators could be useful. For instance, drugs able to specifically chelate iron from iron-containing enzymes such as ribonucleotide reductase or lipoxygenase could find important applications.[4] Moreover, in addition to systemic iron overload, local iron homeostasis disturbances can occur in several conditions associated with so-called ''oxidative stress'', i.e. when traces of iron are locally released from their normal storage sites and become available to catalyze Fenton chemistry, leading to oxidative damage to surrounding biological molecules.[5] However, there are few reports on the development of iron chelators specifically designed for the treatment of such oxidative stress-associated situations. The main reason is probably that the design of such systems is potentially problematic for medicinal chemists in terms of safety margins owing to the possible interaction of chelators with normal iron metabolism.[6]

We recently developed a new strategy based on the idea that an ''ideal'' iron chelator for use in oxidative stress-related conditions should effectively chelate iron only in pro-oxidant conditions. We therefore explored the possibility of generating pro-drugs that can be oxidatively activated into species with strong iron-binding capacity.[7] Of particular interest in such a strategy is the degree of control exercised by the oxidative stress conditions, whereby a dormant relatively inactive compound is transformed to an active species by the very conditions prevailing at sites where it is most needed.

N,*N*′-Bis(3,4,5-trimethoxybenzyl)ethylenediamine-*N*,*N*′-diacetic acid (**L1**) (Figure 1) is the most extensively studied ligand in this series. In aqueous solutions containing acetate and ferric salts, **L1** forms a μ-acetato μ-oxo diferric iron complex.[8] In the presence of ferrous salts in anaerobic conditions, a mononuclear ferrous complex is formed. Both complexes react with hydrogen peroxide or dioxygen in the presence of ascorbate to form a mononuclear (phenolato)-Fe^{III} complex resulting from the quantitative hydroxylation of **L1** into **L5** (Figure 2). Owing to the well-known affinity of phenolate ligands for ferric iron, **L1** appears to fit the aforementioned prerequisites regarding the generation of a strong iron chelator according to a local oxidative activation process.[9]

[a] Laboratoire de Chimie Biomimétique, LEDSS, UMR CNRS 5616, Université J. Fourier
B. P. 53, 38041 Grenoble, Cedex 9, France
E-mail: Guy.Serratrice@ujf-grenoble.fr
[b] Laboratoire d′Electrochimie Organique et de Photochimie Redox, UMR CNRS 5630, Université J. Fourier,
B. P. 53, 38041 Grenoble, Cedex 9, France
[c] Département Molécules & Matériaux, l'OREAL Recherche Avancée,
1 Avenue Eugène Schueller, 93600 Aulnay sous Bois, France

  1434–1948/01/0202–0471 $ 17.50+.50/0

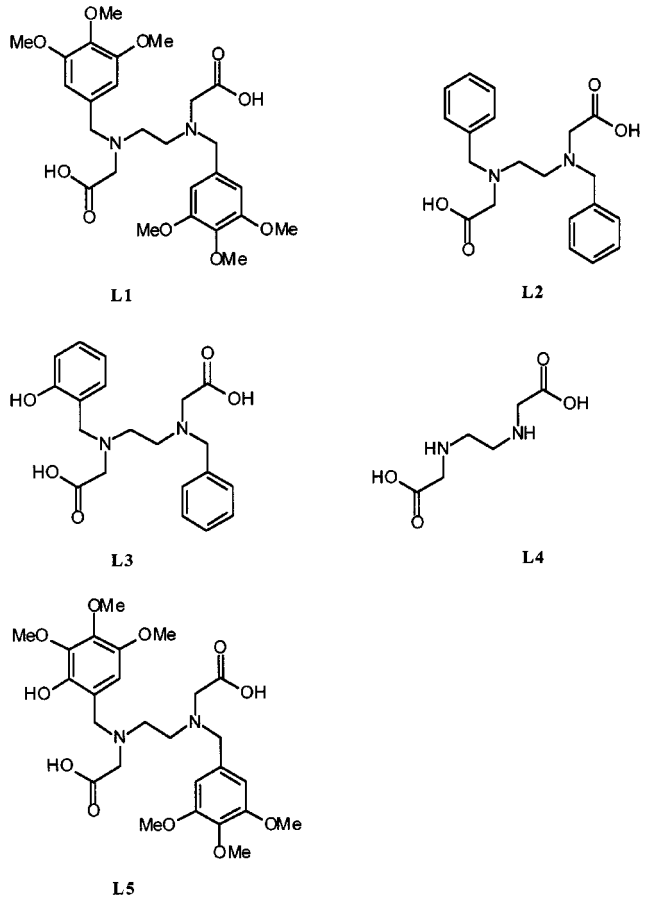

Figure 1. Structure of the ligands **Ln**

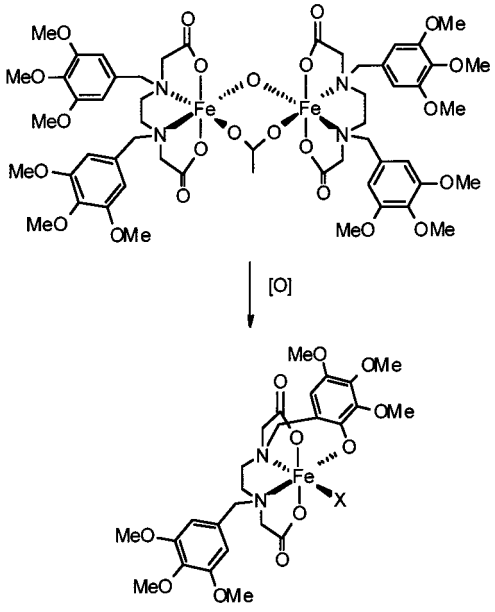

Figure 2. Reaction scheme for the oxidation of $Fe_2(\mathbf{L1})_2$

In the present paper, we extend our previous findings by accurately investigating the physicochemical parameters of Fe^{III} complexation by **L1** and analogs **L2** (*N*,*N*′-dibenzylethylenediamine-*N*,*N*′-diacetic acid) and **L3** [*N*-(2-hydroxybenzyl)-*N*′-benzylethylenediamine-*N*,*N*′-diacetic acid] (Figure 1), i.e. stability constants and redox potentials to demonstrate the pertinence of the use of such ligands to protect biological tissues against iron-catalyzed oxidative damage. The ligand ethylenediamine-*N*,*N*′-diacetic acid (**L4**) was also investigated for comparison and because the stability constants of the ferric complexes are unknown. A detailed kinetic study of the formation and of the dissociation of the ferric complex with **L3** is also described in order to (i) determine the reactivity patterns of this complex containing phenolate and aminoacetate donor groups and (ii) since few data are available in the literature for this type of ligand.

Results and Discussion

Ligand Deprotonation Constants

The deprotonation constants K_a of the ligands investigated in this research were studied by potentiometric titration. Analysis of the potentiometric titration curve (Figure 3a and Figure 3c as examples) by the SUPERQUAD program[10] yielded the pK_{an} values defined by Equation (1) and Equation (2) (charges omitted for clarity) and reported in Table 1.

$$LH_n \rightleftharpoons LH_{n-1} + H^+ \quad (1)$$

$$K_{an} = [LH_{n-1}]\cdot[H^+]/[LH_n] \quad (2)$$

Three pK_a values were determined and these correspond to one carboxylic acid group and the two ammonium groups. By comparison to EDTA the lowest pK_a value for each ligand is attributed to a carboxylic acid and the two highest ones to the ammonium nitrogen atoms. The pK_a values of **L4** are in good agreement with those determined by Harris and Martell [9.67, 6.57 and 2.36 (I = 0.1 M, KNO_3)].[11] The pK_a value of the other carboxylic acid is assumed to be significantly lower than 2.

A fourth pK_a value corresponding to the hydroxy group was determined for the ligand **L3** by spectrophotometric titration. This pK_a cannot be accurately determined by potentiometric titrations since deprotonation occurs at pH > 11. A spectrophotometric titration was carried out over the pH range 10−12. The corresponding UV spectra exhibit an isosbestic point at λ = 270 nm, indicating the presence of only two absorbing species. The data were processed by the LETAGROP SPEFO[12,13] program (absorbance values at 8 wavelengths). The best fit [$\Sigma(A_{exp} - A_{calc})^2 = 10^{-3}$] yielded a p$K_a$ value of 12.0 ± 0.1. The extinction coefficients were determined to be ε_{max} = 3500 $M^{-1}cm^{-1}$ (λ_{max} = 292 nm) and ε_{max} = 10000 $M^{-1}cm^{-1}$ (λ_{max} = 238 nm) for $\mathbf{L3}^{3-}$ and ε_{max} = 50 (λ_{max} = 292 nm) and ε_{max} = 1000 $M^{-1}cm^{-1}$ (λ_{max} = 238 nm) for $\mathbf{L3H}^{2-}$. The pK_a values for **L3** are close to those obtained for the ligands HBIDA [*N*-(2-hydroxybenzyl)iminodiacetic acid][14] and HBED [*N*,*N*′-bis(2-hydroxybenzyl)ethylenediamine-*N*,*N*′-diacetic acid][15] bearing similar donor groups, as indicated in Table 1. The high basicity of the hydroxy group reflects the presence of a hydro-

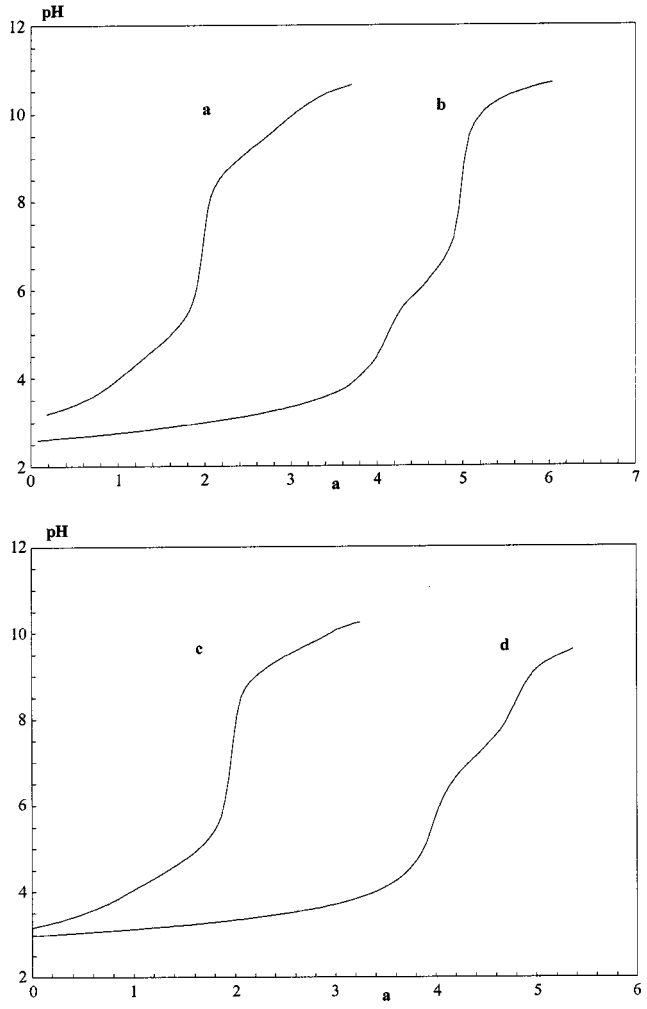

Figure 3. Potentiometric titration curves for (a) 1 mM ligand **L3**; (b) **L3** + Fe^{3+} 1:1, 1 mM; (c) 1 mM ligand **L1**; (d) **L1** + Fe^{3+} 1:1, 1 mM; a = mol of base added per mol of ligand; all solutions were at 25 °C and I = 0.1 M ($NaClO_4$); the data were refined by the SUPERQUAD program (σ_{fit} = 3.5−4.5)

Table 1. Deprotonation constants of the ligands

pK_{an} [a]	L1	L2	L3	L4	HBIDA[b]	HBED[c]
pK_{a1}	9.44(1)	9.68(1)	12.0(1)	9.75(1)	11.71	12.35
pK_{a2}	4.61(2)	4.93(1)	9.11(1)	6.68(2)	8.07	12.08
pK_{a3}	2.87(2)	2.29(3)	4.67(1)	2.64(3)	2.34	8.46
pK_{a4}			2.17(2)			4.76
pK_{a5}						2.18

[a] All values were determined at 25 °C and I = 0.1 M ($NaClO_4$); values in parentheses are standard deviations in the last significant digit. − [b] *N*-(2-Hydroxybenzyl)iminodiacetic acid, ref.[14] − [c] *N*,*N*′-Bis(2-hydroxybenzyl)ethylenediamine-*N*,*N*′-diacetic acid, ref.[15]

gen bond between the amino nitrogen atom and the hydroxy group.

Stability Constants of the Ferric Complexes

The stability constants β_{110} were determined by potentiometric titration for the ferric complexes of ligands **L1**, **L2** and **L4**. The titration curves for a 1:1 ratio of Fe^{III} to ligand (Figure 3d as an example) exhibit two breaks at a = 4 and a = 5, where a is equal to the number of moles of base added per mole of ligand. This clearly indicates the formation of hydroxo complexes Fe(OH)L and $Fe(OH)_2L$ at relatively low pH values. Analysis of the titration curves by the SUPERQUAD program[10] yielded the β_{110} and K^n_{OH} (n = 1 or 2) constants expressed as in Equation (3) and Equation (4).The values are given in Table 2.

$$\beta_{110} = [FeL]/[Fe^{3+}]\cdot[L] \quad (3)$$

$$K^n_{OH} = [Fe(OH)_nL]\cdot[H^+]/[Fe(OH)_{n-1}L] \quad (4)$$

Table 2. Fe^{III}−ligand stability constants and pFe values

Constants[a]	L1	L2	L3	L4
$\log \beta_{110}$	13.95(4)	15.20(9)	27.00(8)[b]	15.50(1)
pK^1_{OH} [c]	3.34(4)	3.52(9)	5.76(8)[b]	3.64(5)
pK^2_{OH} [d]	7.34(5)	7.27(5)		7.18(2)
pFe[e]	17.2	18.1	23.3	18.2

[a] All values were determined at 25 °C and I = 0.1 M ($NaClO_4$); values in parentheses are standard deviations in the last significant digit. − [b] Determined from spectrophotometric titration; K^1_{OH} = 6.02 from potentiometric titration. − [c] $K^1_{OH} = [Fe(OH)L][H^+]/[FeL]$ for the equilibrium $FeL + H_2O \rightleftarrows Fe(OH)L + H^+$. − [d] $K^2_{OH} = [Fe(OH)_2L][H^+]/[Fe(OH)L]$ for the equilibrium $FeLOH + H_2O \rightleftarrows Fe(OH)_2L + H^+$. − [e] Calculated for $[L]_{tot} = 10^{-5}$ M, $[Fe]_{tot} = 10^{-6}$ M at pH = 7.4.

For the tetraprotonated ligand **L3**, the breaks at a = 4 and a = 5 indicate the formation of the FeL and Fe(OH)L complexes (Figure 3b). However, it was not possible to determine the β_{110} value since the formation of the complex is complete at low pH values. Only the value of K^1_{OH} was determined from titration data and this is given in Table 2. The spectrophotometric titration was carried out over the range pH = 1−8 in order to determine the constants β_{110} and K^1_{OH}. The stoichiometric addition of Fe^{III} to a solution of **L3** over the pH range 1−2 led to the formation of a purple complex, the UV/Vis spectrum of which shows a maximum at 525 nm that is attributed to a phenolato-to-Fe^{III} charge transfer transition (Figure 4a). The absorbance data were processed with the LETAGROP-SPEFO program.[12,13] The best fit [$\Sigma(A_{exp} - A_{calc})^2 = 2 \times 10^{-3}$] was obtained by considering the formation of the [FeL] species and provides the values $\log \beta_{110}$ = 27.0 ± 0.08 and ε_{max} = 1950 $M^{-1}cm^{-1}$ (λ_{max} = 520 nm). No spectral change was observed over the pH range 2.5−4.5. As the pH value was increased from 5 to 7, the spectra showed isosbestic points at 394 and 491 nm, indicating that there are only two species with a different absorption in this pH range (Figure 4b). These absorbance data were also refined with the LETAGROP-SPEFO program.[12,13] The best fit [$\Sigma(A_{exp} - A_{calc})^2 = 3 \times 10^{-3}$] showed that deprotonation occurs through a one-proton step yielding a pK^1_{OH} value of 5.76 ± 0.08 and an absorption maximum at λ = 470 nm with ε = 1800 $M^{-1}cm^{-1}$ for the Fe(OH)L species. The value of pK^1_{OH} is in good agreement with the value 6.02 determined by potentiometric titration. The shift of the absorption

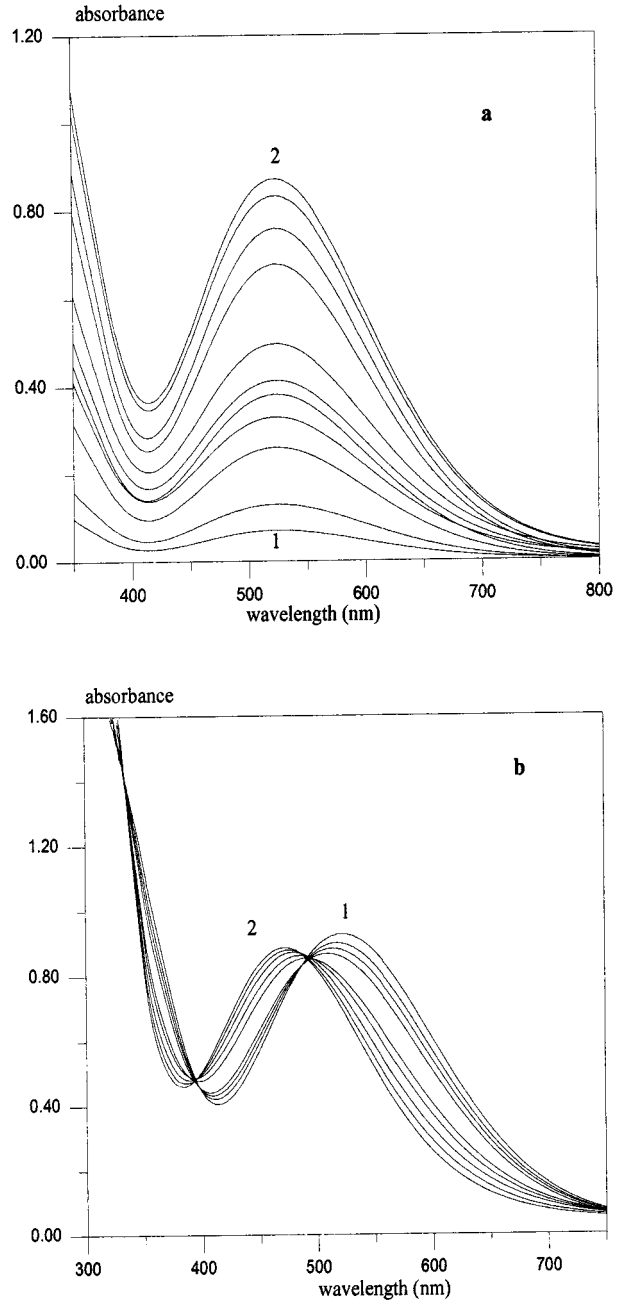

Figure 4. UV/Vis absorption spectra of Fe^{3+}−**L3** as a function of pH; (a) 1: pH = 0.9; 2: pH = 1.8; (b) 1: pH = 4.5; 2: pH = 6.5; $[Fe^{3+}]$ = [**L3**] = 0.5 mM; I = 0.1 M ($NaClO_4$)

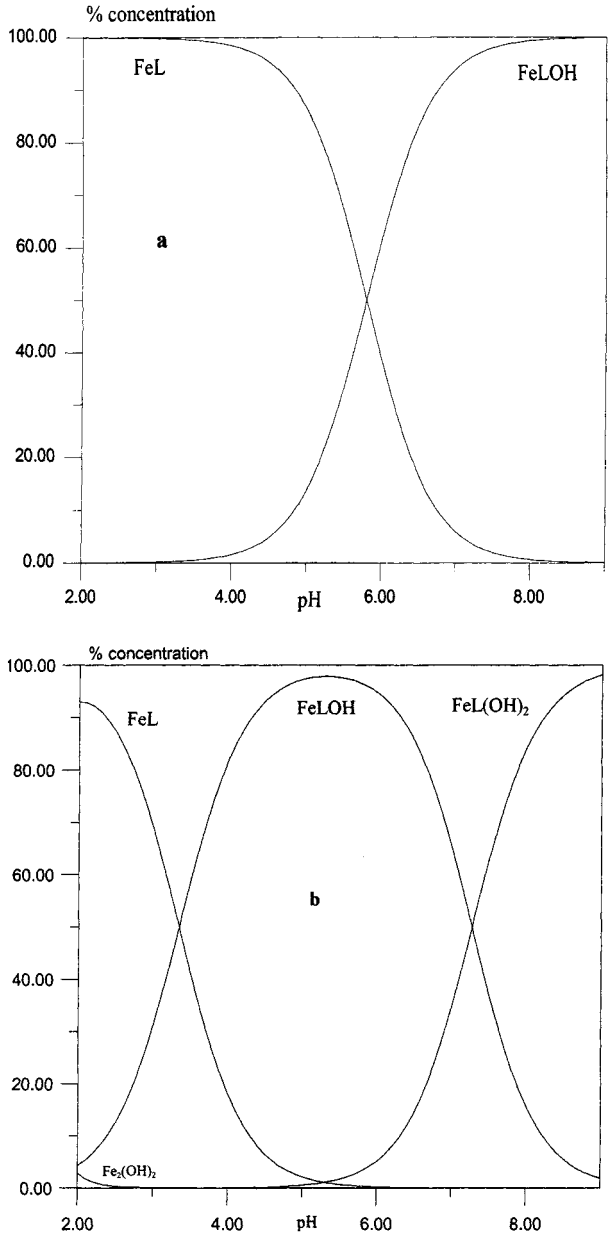

Figure 5. Distribution diagrams of the system Fe^{III}−**L3** (a) and Fe^{III}−**L1** (b) as a function of pH; $[Fe^{3+}]$ = 1 mM, [ligand] = 10 mM

maximum to lower wavelength reflects coordination with the more basic hydroxide ion. A similar spectral change has been observed for the ferric complex with HBIDA[14] [λ_{max} = 518 nm, ε_{max} = 1100 $M^{-1}cm^{-1}$ for FeL, λ_{max} = 460 nm, ε_{max} = 1010 $M^{-1}cm^{-1}$ for Fe(OH)L]. It is worth noting that the extinction coefficient is about half the value for Fe-HBED[15] (λ_{max} = 485 nm, ε_{max} = 3935 $M^{-1}cm^{-1}$), a system that has two phenolate donors and the same framework as **L3**. The distribution curves are shown in Figure 5 for ligands **L1** and **L3**.

The ferric complexes of the tetradentate ligands **L1**, **L2** and **L4** exhibit relatively low stability constants β_{110}, in agreement with those of tetradentate *N*,*N*′-diethylenediamine diacetic acid derivatives. Consequently, low values for pK^1_{OH} are observed (over the range 3.2−3.6). This reflects the high Lewis acid character of the ferric ion in FeL resulting from the low basicity of these ligands. A more reliable parameter for comparison of ligand effectiveness is the pFe^{III} value (= −log $[Fe^{3+}]$). The larger the pFe value, the more effective the ligand. The pFe^{III} values were calculated for $[L]_{tot} = 10^{-5}$ M, $[Fe]_{tot} = 10^{-6}$ M at pH = 7.4 and are reported in Table 2. The pFe values for **L2** and **L4** are very similar, indicating that substitution with benzyl groups does not influence the complexation. The lower ferric affinity of **L1** in comparison to **L2** and **L4** is probably due to steric effects of the methoxy substituents. A higher metal ion affinity is observed for **L3** and this fact is related to the

phenolate donor, as one would expect. An increase in the pFe value of 5.2 from **L2** (18.1) to **L3** (23.3) is observed. A comparison with the hexadentate ligand HBED (pFe = 26.97),[15] which contains two phenolate donors with an EDTA-type framework, shows that incorporation of one phenolate donor increases the pFe value by about 4−5 units. Furthermore, the pFe value for **L3** is higher than that of the tetradentate ligand HBIDA (19.95), which has one phenolate donor, one nitrogen donor and two carboxylate donors. The pK^1_{OH} values are very close, being 5.76 for **L3** and 5.75 for HBIDA. This indicates that the Lewis acidity of Fe^{III} is similar in both complexes.

Electrochemistry

The electrochemical behavior of the Fe^{III} + **L(1−3)** complexes was studied by cyclic voltammetry in an aqueous solution over the pH range 3−10.5 in order to investigate the ability of these complexes to undergo redox cycling under physiological conditions and to catalyze Fenton chemistry. In order to be able to catalyze the formation of hydroxyl radicals in the presence of hydrogen peroxide, an iron complex has to meet two conditions simultaneously: (i) the ferric chelate has to be reducible by physiological reductants, i.e. its standard redox potential must be higher than −0.534 V vs. Ag/AgCl (NADPH/$NADP^+$ redox couple) and (ii) single electron transfer from the ferrous chelate to hydrogen peroxide must be possible, i.e. its redox potential must lie below 0.25 V vs. Ag/AgCl (H_2O_2/HO˙, OH^-). The electrochemical response of the Fe^{III} + **L3** electrolytic solution is characterized in the 3−5 pH range by a quasi-reversible redox wave at $E_{1/2}$ = −0.21 V vs. Ag/AgCl (ΔE_p = 0.12 V, v = 0.1 V s^{-1}) corresponding to the Fe^{III}/Fe^{II} redox couple (Figure 6, curve 1). Increasing the pH value from 5 to 8 results in the progressive appearance of a new redox peak system at $E_{1/2}$ = −0.48 V (ΔE_p = 0.31 V), which grows at the expense of the original one at $E_{1/2}$ = −0.21 V (Figure 6, curves 2−4). Above pH = 8, the original wave disappears and the new peak system reaches full development (Figure 6, curves 5 and 6). This result is in agreement with the pK^1_{OH} value of 5.76 found for the Fe**L3**/Fe(OH)**L3** system and the distribution curve in Figure 5 (see above), i.e. the wave at $E_{1/2}$ = −0.48 V can be attributed to the Fe^{III}(OH)**L3**/Fe^{II}**L3** redox couple. Therefore, at pH = 7.4, the **L3** ferric chelate appears to be mainly in a form that is reducible by physiological reductants. However, the small difference between the $E_{1/2}$ values of NADPH and the **L3** ferric chelate could explain the fact that **L3**−iron is not a catalyst of reductant-driven Fenton reaction under physiological conditions.[7] In addition, a small proportion of the complex remains in the Fe**L3** form, which could be reduced by physiological reductants. This process would allow potential redox cycling of iron, especially during acidosis, which is generally associated with cell oxidative stress. Therefore, it is likely that additional parameters, such as the kinetics of complex formation, compensate for the thermodynamic factor that is favorable for the catalysis of Fenton chemistry.

In contrast, the electrochemical behavior of **L(1−2)** + Fe^{III} complexes appears more complicated, possibly due to the presence of several species in solution at basic pH values, including the μ-oxo binuclear species already characterized by ESI-MS.[8] At pH values above 8, an ill-behaved peak system is seen in the CV curves (Figure 7, curves 1 and 2) (E_{pc} = −0.80 and −0.72 V, E_{pa} = −0.15 and −0.04 V for the complexes **L2** + Fe^{III} and **L1** + Fe^{III}, respectively). For pH values lower than 4.5 (Figure 7,

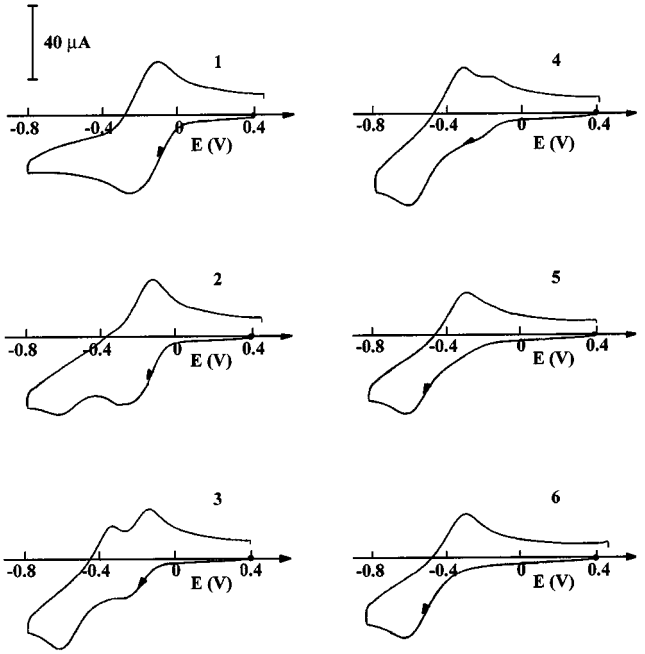

Figure 6. CV curves of Fe^{III} + **L3** (2.9 mM) in H_2O + $NaClO_4$ 0.1 M at a GC electrode (5 mm diameter); scan rate 0.1 Vs^{-1}; E vs. Ag/AgCl, aqueous NaCl (3 M) (+ 0.21 V vs. NHE); pH = 4.2 (1), 5.4 (2), 6.3 (3), 7.0 (4), 8.3 (5), 9.2 (6) (adjusted with $HClO_4$ or NaOH)

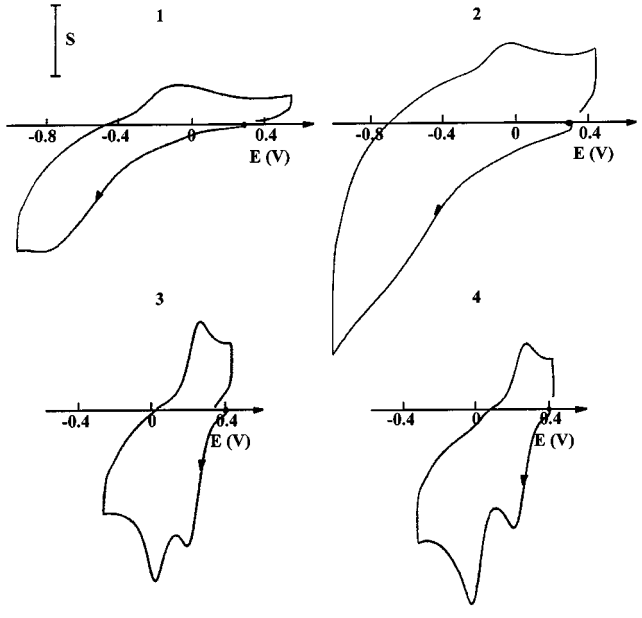

Figure 7. CV curves of Fe^{III} + **L2** (1, 3) and Fe^{III} + **L1** (2, 4), 0.5 mM in H_2O + $NaClO_4$ 0.1 M at a GC electrode (5 mm diameter); scan rate 0.1 V s^{-1}; E vs. Ag/AgCl, aqueous NaCl (3 M) (+0.222 V vs. NHE); pH = 8.3 (1, 2), 3.0 (3, 4) (adjusted with $HClO_4$ or NaOH); scale (S) = 10 μA (1, 2), 4 μA (3, 4)

curves 3 and 4), a reversible redox wave is seen at $E_{1/2}$ = 0.21 and 0.22 V (ΔE_p = 0.06 and 0.08 V, respectively) in the CV curves recorded in the presence of **L2** + Fe^{III} and **L1** + Fe^{III}, respectively. At lower potentials, a fully irreversible peak at 0 V (**L2** + Fe^{III}) or −0.04 V (**L1** + Fe^{III}) is observed, confirming the presence in solution of two different Fe^{III} species in a frozen equilibrium, i.e. the interconversion of these species is slow on the time scale of voltammetry. Between pH = 5 and 8, the CV curves consist of the overlapped electrochemical signals observed in basic and acidic media. These results are in agreement with pK^1_{OH} and pK^2_{OH} values of ca. 3 and 7 found for both **L2** + Fe^{III} and **L1** + Fe^{III} complexes, i.e. in basic media only the $Fe^{III}(OH)_2L$ complex is present in solution whereas in acidic media an equilibrium between $Fe^{III}L$ and $Fe^{III}(OH)L$ occurs. Taking into account the negative shift in potential for the redox couple $Fe^{III}(OH)L/Fe^{II}L$ in comparison to Fe^{III}**L3**/Fe^{II}**L3**, it can be assumed that the reversible wave at around 0.2 V is attributable to the $Fe^{III}L/Fe^{II}L$ redox couple (where L signifies **L1** or **L2**) when the irreversible electron transfer corresponds to the cathodic process characteristic of Fe^{III}(OH)**L3**. The irreversibility of the electron transfer is likely to be due to a change in the coordination sphere around the Fe center upon reduction. Comparing **L1** and **L2**, it must be noted that the substitution of **L1** with electron-donating methoxy groups does not influence significantly the potential characteristic of the iron-localized electron transfer. In addition, under the same experimental conditions, $E_{1/2}$ for the Fe^{III}EDTA/Fe^{II}EDTA redox couple is found at −0.10 V, showing that **L3** stabilizes the Fe^{III} form of the complex by ca. 0.12 V while **L1** and **L2** stabilize the Fe^{II} form of the complex by ca. 0.31 V. This is in agreement with the presence of the hard coordinating hydroxo site on **L3**.

Formation and Acid Hydrolysis Kinetics of the FeL3 Complex

The capacity of a chelator to protect against the formation of damaging oxidizing species is influenced not only by several thermodynamic factors, but also by kinetic factors. Therefore, the kinetics of formation of the Fe**L3** complex was investigated by a stopped-flow spectrophotometric method under pseudo-first-order conditions: [Fe^{III}] and [H^+] >> [L] and at ionic strength I = 2 M, 25 °C. The absorbance change vs. time of the phenolato-to-Fe^{III} charge transfer band at λ = 525 nm showed a single exponential curve indicating that the complex formation reaction proceeds through a single rate-limiting step. The spectra recorded with time using a diode array device were similar to those shown in Figure 4a. It was found that the pseudo first-order rate constants k_{obs} at a given acidity level ([H^+] varied from 0.05 to 0.15 M) have a linear variation as a function of [Fe^{3+}] with a significant intercept (Figure 8) that indicates a contribution of the reverse reaction. The slopes of these plots decrease as [H^+] increases. In addition, the intercepts of the plots increase as [H^+] increases.

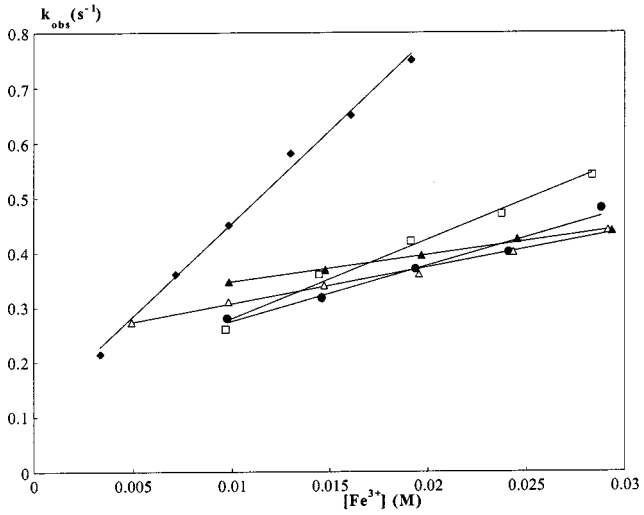

Figure 8. Variation of the experimental rate constant k_{obs} (s^{-1}) for the formation of the Fe^{III}−**L3** complex as a function of [Fe^{3+}] (M) at various [H^+] (M): (◆) 0.05, (□) 0.08, (●) 0.10, (Δ) 0.125, (▲) 0.15; [**L3**] = 0.4 mM; solvent: water, I = 2.0 M ($HClO_4$ + $NaClO_4$), T = 25 °C

The acid hydrolysis kinetics of the Fe−**L3** complex was studied in aqueous solution (ionic strength I = 2 M, 25 °C) by the pH jump method. The pH jump reactions were performed under pseudo-first-order conditions with respect to [H^+] (varying over the range 0.02−0.9 M) for solutions containing Fe^{III} and **L3** in a 1:1 molar ratio at an initial pH value of 4. The UV/Vis spectra recorded as a function of the time resemble the spectra recorded for the formation reaction study and for the equilibrium study at pH < 2 (Figure 4a) and indicate a total dechelation at the iron center. The exponential absorbance decay vs. time recorded at 520 nm indicates that the dissociation occurs through a single determining step. The plot of the k_{obs} rate constants vs. [H^+] is linear over the [H^+] range 0.2−1.0 M and slightly curved at low [H^+] (Figure 9).

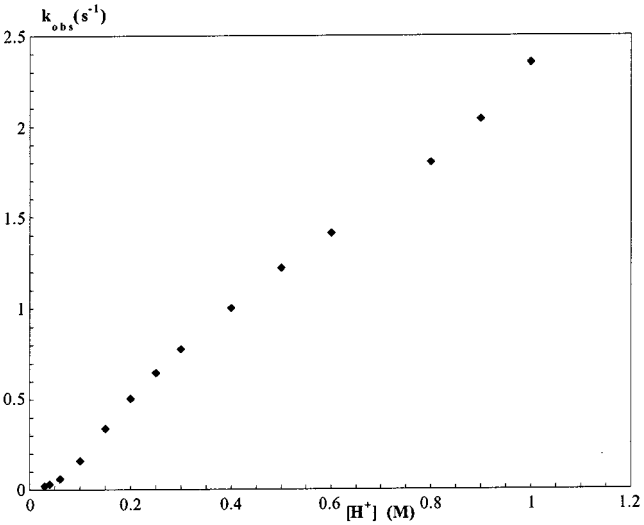

Figure 9. k_{obs} (s^{-1}) as a function of [H^+] (M) in the acid hydrolysis kinetics of the Fe^{III}−**L3** complex, [Fe**L3**] = 0.5 mM; solvent: water; I = 2.0 M ($HClO_4$ + $NaClO_4$), T = 25 °C

By taking into account the equilibria existing in solution under the experimental conditions and after analyzing the kinetics results from both the formation and the hydrolysis reactions, the reaction scheme shown in Equation (5) to Equation (14) can be proposed ($[FeOH]^{2+}$ for $[Fe(OH)(OH_2)_5]^{2+}$, Fe^{3+} for $[Fe(OH_2)_6]^{3+}$ and L for **L3**).

$$Fe^{3+} \rightleftharpoons FeOH^{2+} + H^+ \qquad K_{Fe} \qquad (5)$$

$$LH_5^{2+} \rightleftharpoons LH_4^+ + H^+ \qquad K_{a5} \qquad (6)$$

$$LH_4^+ \rightleftharpoons LH_3 + H^+ \qquad K_{a4} \qquad (7)$$

$$Fe^{3+} + LH_5^{2+} \rightleftharpoons FeLH_2^{3+} + 3\,H^+ \qquad k_0, k_{-0} \qquad (8)$$

$$FeOH^{2+} + LH_5^{2+} \rightleftharpoons FeLH_2^{3+} + 2\,H^+ + H_2O \qquad k_1, k_{-1} \qquad (9)$$

$$Fe^{3+} + LH_4^+ \rightleftharpoons FeLH_2^{3+} + 2\,H^+ \qquad k_2, k_{-2} \qquad (10)$$

$$FeOH^{2+} + LH_4^+ \rightleftharpoons FeLH_2^{3+} + H^+ + H_2O \qquad k_3, k_{-3} \qquad (11)$$

$$Fe^{3+} + LH_3 \rightleftharpoons FeLH_2^{3+} + H^+ \qquad k_4, k_{-4} \qquad (12)$$

$$FeOH^{2+} + LH_3 \rightleftharpoons FeLH_2^{3+} + H_2O \qquad (13)$$

$$FeLH_2^{3+} \rightleftharpoons FeL^+ + 2\,H^+ \qquad K_{FeLH2} \qquad (14)$$

It was assumed that the rate-determining pathway involves the formation of the $[FeLH_2^{3+}]$ complex since the reaction proceeds through the coordination of Fe^{3+} with the phenolato oxygen atom and releases only one H^+ in the reaction according to Equation (12).

The pseudo-first-order kinetic according to Equation (15) can be obtained by neglecting terms from reactions according to Equation (8) to Equation (10), in agreement with the experimental results, where $[Fe^{3+}] = [Fe^{3+}]_{tot} - [FeOH^{2+}] - 2\,[Fe_2(OH)_2^{4+}]$ and $[H^+]$ takes into account the protons involved in formation of $[FeOH]^{2+}$ and $[Fe_2(OH)_2]^{4+}$ ($2\,Fe^{3+} \rightleftarrows [Fe_2(OH)_2]^{4+} + 2\,H^+$, K_{DFe}).

$$k_{obs} = \frac{[Fe^{3+}]}{[H^+]([H^+]^2 + [H^+]K_{a5} + K_{a4}K_{a5})}\{(k_3K_{Fe}K_{a5} + k_4K_{a4}K_{a5})[H^+] + k_5K_{Fe}K_{a4}K_{a5}\} + \{(k_{-3} + k_{-4})[H^+] + k_{-5}\}\left(\frac{[H^+]^2}{[H^+]^2 + K_{FeLH2}}\right) \qquad (15)$$

The values of K_{Fe} and K_{DFe} in 2.0 M $NaClO_4$ are 1.5×10^{-3} M and 2.4×10^{-3} M.[16] Since pK_{a5} was not determined, the fit of the data was performed using the value 1.17, which was obtained for the corresponding deprotonation of HBED.[15] The variation of the pseudo-first-order kinetic rate constant of the hydrolysis reaction is consistent with the last term of Equation 15.[17] The results of the nonlinear least-squares fit to Equation (15) of the combined formation and dissociation data are:

$(k_3K_{Fe}K_{a5} + k_4K_{a4}K_{a5}) = 0.078 \pm 0.018\ M^{-1}s^{-1}$ $k_5 = 13300 \pm 1400\ M^{-1}s^{-1}$

$(k_{-3} + k_{-4}) = 1.83 \pm 0.09\ M^{-1}s^{-1}$ $k_{-5} = 0.42 \pm 0.08\ s^{-1}$ $K_{FeLH2} = 0.026 \pm 0.005\ M^2$

The rate constants of the Fe^{3+} pathways have been found to be generally almost three orders of magnitude lower than those of the $[FeOH]^{2+}$ pathways.[18] So, if we assume a value of about $10\ M^{-1}s^{-1}$ for k_4, it seems reasonable to neglect the $k_4K_{a4}K_{a5}$ term with respect to $k_3K_{Fe}K_{a5}$. Thus, we can obtain $k_3 = 770 \pm 180\ M^{-1}s^{-1}$. From the values of k_5 and k_{-5}, $k_4/k_{-4} = K_{Fe}\,k_5/k_{-5}$ is calculated to be 47.5. An upper limit of k_{-4} is thus estimated to be 0.2 if $k_4 < 10$ and so we can obtain $k_{-3} = 1.6\ s^{-1}$.

In summary, we were able to determine the following rate constants:

$k_5 = 13300 \pm 1400\ M^{-1}s^{-1}$; $k_{-5} = 0.42 \pm 0.08\ s^{-1}$

$k_3 = 770 \pm 180\ M^{-1}s^{-1}$; $k_{-3} = 1.6 \pm 0.1\ s^{-1}$

Ligand substitution reactions at an iron center were assumed to be controlled by water exchange from the inner coordination shell. The rate constants may be described according to the Eigen−Wilkins mechanism[19] with a fast formation step of an outer-sphere complex (K_{os}) followed by a rate-limiting step involving the water substitution of the $[FeOH]^{2+}$ species (k_{ex}) according to Equation (16); k_f stands for k_3 or k_5, S is a statistical coefficient that accounts for the solvent shell composition and can be assigned an approximate value of 1/6.

$$k_f = K_{os} \cdot S \cdot k_{ex} \qquad (16)$$

Since k_{ex} does not change significantly with different ligands, variations in the rate constants are mainly due to the constant K_{os}. The charge of the ligand is one of the factors that influences the value of K_{os}. The constant can be estimated with the Fuoss equation[20] to be 0.2 for reactions of $[FeOH]^{2+}$ with a neutral ligand and ca. 0.02 for a ligand bearing a global positive charge. Accordingly, the value of k_5, which refers to the $[FeOH]^{2+} - LH_3$ pathway, is larger than the value of k_3, which refers to the $[FeOH]^{2+} - LH_4^+$ pathway ($k_5/k_3 \approx 17$). Furthermore, a comparison with the literature data indicates that k_5 is much higher than the rate constants determined for the $[FeOH]^{2+}$ − neutral ligand pathway for phenol, catechol and hydroxamate ligands (about 1×10^3 to $3 \times 10^3\ M^{-1}s^{-1}$). This finding can be explained by taking into account the zwitterionic character of the ligand **L3**. The two carboxylate anions are assumed to increase the K_{os} constant with respect to a ligand bearing no charges. The values of k_5 fall within the range for a ligand containing one or two aminoacetate donor groups,[21] such as H_4EDTA ($30000\ M^{-1}s^{-1}$) and H_3NTA ($15000\ M^{-1}s^{-1}$).

Kinetic data for the dissociation of ferric complexes with this type of ligand are not available in the literature. A comparison can be made with dissociation rate constants obtained for catecholate and hydroxamate ligands, which are the most widely reported in the literature. The dissociation rate of Fe**L3** by the $[FeOH]^{2+}$ pathway (1.6 and $0.42\ s^{-1}$) is close to that of the (monocatecholato)Fe−Tiron (1,2-dihydroxy-3,5-benzenedisulfonate) complex ($1.2\ s^{-1}$)[22] but significantly faster than those of the monohydroxamato

complexes (0.08 s^{-1} for acetohydroxamic acid and 0.0071 s^{-1} for *N*-methylacetohydroxamic acid).[23,24] A comparison with the last step of the dissociation of hexadentate chelates shows that **L3** releases Fe^{III} much faster than the tricatecholate TRENCAMS[25] (0.018 s^{-1}) and than the siderophores pyoverdin[26] ($> 6\ 10^{-5}\ s^{-1}$) and ferrioxamine B[27,28] (0.0021 s^{-1}).

Conclusion

In summary, this work has shown that the bis(aminocarboxylate)benzyl chelators of the present series have a relatively low affinity for Fe^{III}. It must be emphasized that these chelators (except **L3**) should be thermodynamically unable to compete for iron in most metalloproteins and especially for transferrin. For this reason side-effects can be expected to be limited, a situation in contrast to strong iron chelators, which can inhibit enzymes by removal of metal from active sites, by formation of a ternary complex or by depriving the apoenzyme of its normal source of iron. Under prooxidant conditions, e.g. in the presence of hydrogen peroxide, these chelators are hydroxylated to give species with strong iron affinity, as shown by the complexation stability constants and pFe value for **L3**, which are consistent with the presence of a hard phenolate donor group. Moreover, this dramatic increase of affinity for iron is associated with a large decrease in redox potential of Fe^{III}/Fe^{II}, which tends to inhibit iron reduction by physiological reductants thereby avoiding redox cycling of iron. However, it should be kept in mind that such a consideration refers to equilibrium conditions, which is generally not the case in biological systems, and these results agree with previous data showing that the **L3** iron complex is not a catalyst of reductant-driven Fenton reactions.[7] In addition, both the formation and dissociation kinetics of the ferric complex with **L3** were measured and were found to give consistent data. It should be emphasized that an interesting feature of **L3** is the fast uptake of Fe^{III} and its fast release under acidic conditions. The results presented here are in good agreement with biological data showing a very efficient protection of cultured cells by **L3** or **L1** prodrugs against hydrogen peroxide toxicity.[29,9]

Experimental Section

Materials and Equipment: Ligands **L1** and **L2** were prepared according to the procedure described previously.[8] All other compounds were of reagent grade and were used without further purification. Fe^{III} stock solutions were prepared by dissolving appropriate amounts of ferric perchlorate hydrate (Aldrich) in standardized $HClO_4$ and $NaClO_4$ solutions. The solutions were calibrated spectrophotometrically for ferric ions by using a molar extinction coefficient of 4160 $M^{-1}cm^{-1}$ at 240 nm.[30] Mass spectra were obtained by HPLC/MS with a Fisons Platform mass spectrometer equipped with an atmospheric pressure ion source in the electrospray ionization (ESI) mode. ^1H NMR spectra were recorded with a Bruker 500 MHz spectrometer.

Synthesis of L3

(a) *N*-(2-Hydroxybenzyl)-*N*′-benzylethylenediamine: A mixture of 8.05 g (66 mmol) of 2-hydroxybenzaldehyde and 10 g (66.6 mmol) of *N*-benzylethylenediamine was heated in 100 mL of MeOH at 50 °C for 30 min. The mixture was concentrated, the residue suspended in 150 mL of EtOH and 34 mmol of $NaBH_4$ was added. The reaction mixture was stirred at room temperature for 1 h and the solvent evaporated. 100 mL of water was added and concentrated HCl was used to acidify the solution to pH = 1−2. The crystalline dihydrochloride was collected by filtration, washed with cold ethanol and vacuum-dried over P_2O_5 to yield 13.85 g (81%) of *N*-(2-hydroxybenzyl)-*N*′-benzylethylenediamine. − MS (ESI^+); *m*/*z*: 256 $[M + H]^+$, 91 $[C_7H_7^+]$.

(b) *N*-(2-Hydroxybenzyl)-*N*′-benzylethylenediamine Diacetic Acid: A mixture of 12.8 g (50 mmol) of *N*-(2-hydroxybenzyl)-*N*′-benzylethylenediamine, 13.9 g (100 mmol) of bromoacetic acid, 2 g (50 mmol) of NaOH and 8.4 g (100 mmol) of $NaHCO_3$ in 150 mL of water was heated at 40 °C for 6 h while the pH value of the solution was maintained in the range of 11.5−12.5 by the addition of NaOH. Concentrated HCl was added to the reaction mixture until the pH value was lowered to 2. The white precipitate was filtered off and recrystallized from 2-propanol to yield 10 g of *N*-(2-hydroxybenzyl)-*N*′-benzylethylenediamine diacetic acid hydrochloride as a white powder (m.p. 190 °C, yield 46%). − ^1H NMR ([D$_6$]DMSO): δ = 3.14 (t, 2 H), 3.31 (t, 2 H), 3.42 (s, 2 H), 3.90 (2 × s, 4 H), 4.27 (s, 2 H), 6.85 (td, 1 H), 6.95 (d, 1 H), 7.23 (m, 7 H). − $C_{20}H_{25}ClN_2O_5$ (+ 0.05 NaCl) (411.8): calcd. C 58.33, H 6.08, Cl 9.06, N 6.80, O 19.45; found C 58.21, H 6.09, N 6.53, O 19.86, Cl 9.20.

Potentiometric Titrations: All the measurements were made at 25 °C and the solutions were prepared with deionized water that had been distilled twice. The ionic strength was fixed at $I = 0.1$ M with sodium perchlorate (PROLABO puriss). The potentiometric titrations were performed using an automatic titrator system, DMS 716 Titrino (Metrohm), equipped with a combined glass electrode (Metrohm, filled with saturated NaCl solution) and connected to an IBM Aptiva microcomputer. The electrodes were calibrated to read p[H] according to the classical method[31] (from titration of 0.1 M $HClO_4$ by 0.1 M NaOH). The ligand and its iron(III) complex of ca. 0.001 M were titrated with standardized 0.025 M sodium hydroxide. Argon was bubbled through the solutions to exclude CO_2 and O_2. Sodium hydroxide was prepared from 0.1 M NaOH (Prolabo) and was standardized. The titration data (120 points collected over the pH range 2.5−10.5 for the ligand solution and 100 points collected over the pH range 2.5−10 for the Fe^{III}−ligand solution) were refined by the nonlinear least-squares refinement program SUPERQUAD[10] to determine the deprotonation constants (σ_{fit} in the range 3−4). The pK_{an} values were calculated from the cumulative constants determined with the above program. The uncertainties in the pK_{an} values correspond to the standard deviations (1σ) in the cumulative constants.

Spectrophotometric Experiments: UV/Vis absorption spectra were recorded with a Perkin−Elmer Lambda 2 spectrometer using 1.000-cm path-length quartz cells and connected to a microcomputer; the acquisition was made with UV Winlab software (Perkin−Elmer). The temperature was maintained at 25 °C with a Perkin−Elmer PTP-1 variable temperature unit. The ferric complex with **L3** was studied by spectrophotometry. The UV/Vis spectrum of a solution containing equal amounts of ligand and Fe^{III} (10^{-4} M) was recorded as a function of pH over the range 1−8 (adjusted with $HClO_4$ or NaOH). An aliquot was taken from the solution

after each adjustment of the pH value and its spectrum was recorded. The pH measurements were made with a 713 Metrohm digital pH meter equipped with a microelectrode. The ionic strength was fixed at $I = 0.1$ M with $NaClO_4/HClO_4$. The spectrophotometric data were analyzed using the LETAGROP-SPEFO program.[12,13] The program uses a nonlinear least-squares method to calculate the thermodynamic constants of the absorbing species and their corresponding electronic spectra. The calculations were performed using absorbance values from about 6−8 wavelengths (between 400 and 600 nm). The range of values for the residual-squares sum $[\Sigma(A_{exp} - A_{calc})^2]$ of the fits was $10^{-2}-10^{-3}$.

Electrochemical Measurements: Electrochemical experiments were carried out using a PAR model 273 potentiostat equipped with a Kipp−Zonen x-y recorder. All experiments were run at room temperature under argon in a glove-box. A standard three-electrode cell was used. Potentials are referenced to Ag/AgCl, 3 M NaCl, aqueous reference electrode (+0.21 V vs. NHE). A glassy carbon disc electrode, used as a working electrode (5 mm diameter), was polished with 1 μm diamond paste. The electrochemical behavior of the Fe^{III}−ligand complex was studied by cyclic voltammetry (CV) in an aqueous solution containing 0.1 M $NaClO_4$ as a supporting electrolyte and buffered with tris-buffer for the experiments performed at pH = 7. For the experiments performed at pH ≠ 7, the pH value was adjusted following controlled additions of concentrated NaOH or $HClO_4$ aqueous stock solutions. The Fe^{III}−ligand solutions were prepared by dissolving stoichiometric amounts of ferric perchlorate and ligand in the electrolytic solutions.

Kinetics Studies: Kinetic measurements were performed with a KINSPEC UV (BIO-LOGIC Company, Claix, France) stopped-flow spectrophotometer equipped with a diode array detector (J & M) and connected to a TANDON microcomputer. The kinetic data were treated online with the commercial BIO-KINE program (BIO-LOGIC Company, Claix, France). The ionic strength was fixed at $I = 2$ M ($NaClO_4$, $HClO_4$) owing to the H^+ concentrations up to 1 M and allowing comparisons with literature data. − Formation kinetic studies were carried out under pseudo-first-order conditions at 25 °C with Fe^{III} in excess with respect to the ligand. The Fe^{III} concentration spanned the range $5 \times 10^{-3}-3 \times 10^{-2}$ M for each H^+ concentration, which was over the range 0.05−0.15 M. A solution containing Fe^{III} and H^+ and a solution containing the ligand **L3** (2×10^{-4} M) at the same ionic strength were mixed on the stopped-flow apparatus. In each case, first-order kinetics were observed. The reported rate constants are the average of about 8 replicate determinations (standard deviation in the range 1−2%). − The acid hydrolysis kinetics of the Fe^{III}−**L3** complex was studied under pseudo-first-order conditions in the presence of excess protons ($[H^+]$ range 0.02−1.0 M) at 25 °C. The initial pH value of the Fe^{III}−**L3** solution (7×10^{-4} M) was 4.

Acknowledgments

The authors thank Céline Carresi for performing the potentiometric measurements and Arnaud Pierra for performing the UV/Vis spectrophotometric and kinetic measurements with ligand **L3**. We are grateful to Dr. Alain Deronzier (LEOPR, Grenoble, France) for the use of the laboratory facilities, to Professor C. Béguin (LEDSS, Grenoble, France), Professor M. Fontecave and Dr. S. Ménage (CBCRB, CEA, Grenoble, France) for their interest in these studies.

[1] R. C. Hider, S. Singh, *Proc. R. Soc. Edimburgh, Sect. B* **1992**, *99*, 137−168.
[2] R. C. Crichton, In *Inorganic Biochemistry of Iron Metabolism*, Ellis Horwood Ltd., New York, **1991**, p. 173.
[3] C. Herschko, *Mol. Aspects Med.* **1992**, *13*, 114.
[4] J. B. Porter, E. R. Huens, R. C. Hider, *Bailliere's Clin. Haematol.* **1989**, *2*, 257.
[5] B. Halliwell, J. M. C. Gutteridge, *Free Radicals in Biology and Medicine*, 2nd ed., Clarendon Press, Oxford, **1989**.
[6] J.-B. Galey, *Adv. Pharmacol.* **1996**, *38*, 167.
[7] J.-B. Galey, J. Dumats, S. Génard, O. Destrée, P. Pichaud, P. Catroux, L. Marrot, I. Beck, B. Fernandez, G. Barre, M. Seite, G. Hussler, M. Hocquaux, *Biochem. Pharmacol.* **1996**, *51*, 103.
[8] S. Ménage, J.-B. Galey, J. Dumats, G. Hussler, M. Seité, I. Gautier-Luneau, G. Chottard, M. Fontecave, *J. Am. Chem. Soc.* **1998**, *120*, 13370.
[9] J.-B. Galey, O. Destrée, J. Dumats, S. Génard, P. Tachon, *J. Med. Chem.* **2000**, *43*, 1418.
[10] P. Gans, A. Sabatini, A. Vacca, *J. Chem. Soc., Dalton Trans.* **1985**, 1195.
[11] W. R. Harris, A. E. Martell, *Inorg. Chem.* **1976**, *14*, 713.
[12] L. G. Sillen, B. Warsquist, *Ark. Kemi* **1969**, *31*, 377.
[13] M. Meloun, J. Havel, E. Hogfeldt, *Computation of Solution Equilibria*, Ellis Horwood, Chichester, **1988**.
[14] W. R. Harris, A. E. Martell, *Inorg. Chem.* **1975**, *14*, 974.
[15] R. J. Motekaitis, Y. Sun, A. E. Martell, M. J. Welch, *Inorg. Chem.* **1991**, *30*, 2737.
[16] R. M. Milburn, W. C. Vosburgh, *J. Am. Chem. Soc.* **1955**, *77*, 1352.
[17] The term arising from the reverse reaction is negligible under the experimental conditions of the hydrolysis reaction.
[18] M. Birus, N. Kujundzic, M. Pribanic, *Prog. React. Kinet.* **1993**, *18*, 171.
[19] M. Eigen, R. G. Wilkins, *Adv. Chem. Ser.* **1965**, 55.
[20] R. M. Fuoss, *J. Am. Chem. Soc.* **1958**, *80*, 5059.
[21] E. Mentasti, E. Pelizetti, G. Saini, *J. Chem. Soc., Dalton Trans.* **1974**, 1944.
[22] Z. Zhang, R. B. Jordan, *Inorg. Chem.* **1996**, *35*, 1571.
[23] M. Birus, Z. Bradlic, N. Kujundzic, M. Pribanic, P. C. Wilkins, R. G. Wilkins, *Inorg. Chem.* **1985**, *24*, 3980.
[24] M. T. Caudle, A. L. Crumbliss, *Inorg. Chem.* **1994**, *33*, 4077.
[25] F. Thomas, C. Béguin, J.-L. Pierre, G. Serratrice, *Inorg. Chim. Acta* **1999**, *291*, 148.
[26] A.-M. Albrecht-Gary, S. Blanc, N. Rochel, A. Z. Ocaktan, M. A. Abdallah, *Inorg. Chem.* **1994**, *33*, 6391.
[27] B. Monzyk, A. L. Crumbliss, *J. Am. Chem. Soc.* **1982**, *104*, 4921.
[28] M. Birus, Z. Bradlic, G. Krznaric, N. Kujundzic, M. Pribanic, P. C. Wilkins, R. G. Wilkins, *Inorg. Chem.* **1987**, *26*, 1000.
[29] J.-B. Galey, O. Destrée, J. Dumats, P. Pichaud, J. Marché, S. Génard, G. Bracciolli, L. Le Capitaine, H. Plessix, L. Brambilla, O. Cantoni, *Free Rad. Biol. Med.* **1998**, *25*, 881.
[30] R. Bastian, R. Weberling, F. Palilla, *Anal. Chem.* **1956**, *28*, 459.
[31] A. E. Martell, R. J. Motekaitis, *Determination and Use of Stability Constants*, 2nd ed., VCH Publishers, New York, **1992**.

Received May 3, 2000
[I00179]